Mendeleev Communications

Mendeleev Commun., 2025, **35**, 413–416

Carbazole-based conjugated polymers with enhanced UV hardness: promising electron donor materials for stable organic solar cells

Ekaterina A. Komissarova,[a] Sergey A. Kuklin,[a,b] Petr M. Kuznetsov,[a] Al'bert N. Galiullin,[b] Nikita A. Slesarenko[a] and Pavel A. Troshin*[c,a]

[a] *Federal Research Center of Problems of Chemical Physics and Medicinal Chemistry, Russian Academy of Sciences, 142432 Chernogolovka, Moscow Region, Russian Federation. E-mail: troshin2003@inbox.ru*
[b] *A. N. Nesmeyanov Institute of Organoelement Compounds, Russian Academy of Sciences, 119334 Moscow, Russian Federation*
[c] *Zhengzhou Research Institute, Harbin Institute of Technology, 450003 Zhengzhou, China*

DOI: 10.71267/mencom.7708

Guided by the previously discovered relationships between the molecular structure of the conjugated polymers and their photostability, herein, we have successfully designed and synthesized new conjugated polymers incorporating thiophene, 2,1,3-benzotriazole and carbazole units employing the Stille coupling. The polymers exhibited record-high stability under UV light exposure, outperforming a well-known and fairly stable benchmark material, PCDTBT. The presented novel materials can be promising electron-donor components for the new generation of organic solar cells fitting the 'golden triangle', *i.e.*, showing high efficiency, long operational lifetimes, and low cost of the used raw materials.

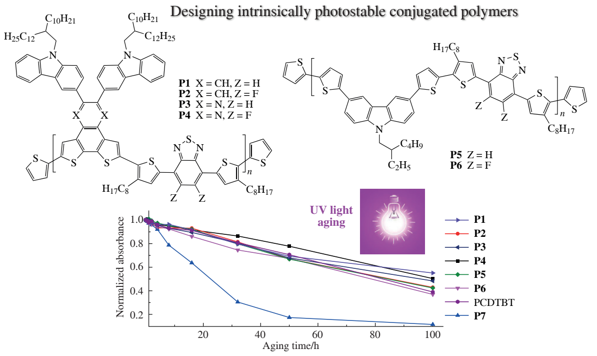

Keywords: conjugated polymers, organic solar cells, photostability, operational stability, UV light hardness, Stille reaction, carbazole.

Organic solar cells represent a highly promising emerging photovoltaic technology with competitive performance characteristics: multiple reports have recently confirmed reaching power conversion efficiencies of 20% and even beyond.[1–3] Therefore, practical implementation of organic solar cells now severely depends on solving the stability issues[4,5] and decreasing the cost of the used organic absorber materials.[6,7] In terms of the cost of raw materials, much simplified synthesis has to be developed, in particular, for non-fullerene acceptor materials.[8,9] Achieving long operational lifetimes of organic solar cells requires deep fundamental understanding of the light-induced degradation behavior of the active materials and rational design of new donor and acceptor compounds with largely improved intrinsic stability.

A series of papers reported the light-induced degradation of conjugated polymers in the presence of oxygen, usually just in air without any special protection, which is not relevant to the realistic solar cell operation conditions when devices have to be thoroughly encapsulated.[10,11] Therefore, more attention has to be paid to the 'intrinsic photostability', which is reflecting how a material behaves upon exposure to light without the involvement of any external factors such as oxygen or moisture.[12,13] We have contributed to the development of tools to assess the intrinsic stability of conjugated polymers and fullerene derivatives using electron spin resonance spectroscopy, impedance measurements, chromatography, *etc*.[14–18] In particular, we have demonstrated that all conjugated polymers and small molecules underwent facile light-induced cross-linking that created energetic disorder in the device active layer and resulted in the burn-in effect, which is the efficiency loss within the first few hundred hours of solar cell operation.[18] To address this problem, we tried to analyze the correlations between the molecular structures of conjugated polymers and their photostability.[19–21] It has been shown, in particular, that incorporation of carbazole units improves UV light hardness of conjugated polymers. Similar observations were made by other researchers at the level of studied materials and also directly in the structure of organic solar cells.[22,23]

Herein, we report the rational design of a series of carbazole-based conjugated polymers and the investigation of their photostability under exposure to the hard UV irradiation. The synthesis of conjugated polymers **P1**–**P6** containing different number of carbazole blocks in the main chain and as side substituents was carried out using palladium-catalyzed Stille polycondensation reaction (Scheme 1). The key monomers **1**, **2** and **3**, **4** were synthesized as reported previously.[24,25] The synthesis of **5** is described in Online Supplementary Materials.

Dynamic gel permeation chromatography (GPC) was used to monitor the progress of the polycondensation reaction. It was found that **P5** had poor solubility in toluene and therefore started to precipitate shortly after initiation of the polycondensation reaction. Therefore, the reaction was intentionally terminated when the polymer molecular weight reached about 9 kDa by the addition first of an excess of 2-(trimethylstannyl)thiophene followed by the introduction of a larger excess of 2-bromothiophene. Similar termination of the reaction in the case of other polymers was performed when the appropriate molecular weight was reached or after the appearance of the first signs of the polymer precipitation (**P1**, **P4**, **P6**).

The obtained crude polymers **P1**–**P6** were purified from low-molecular impurities by extraction in a Soxhlet apparatus using

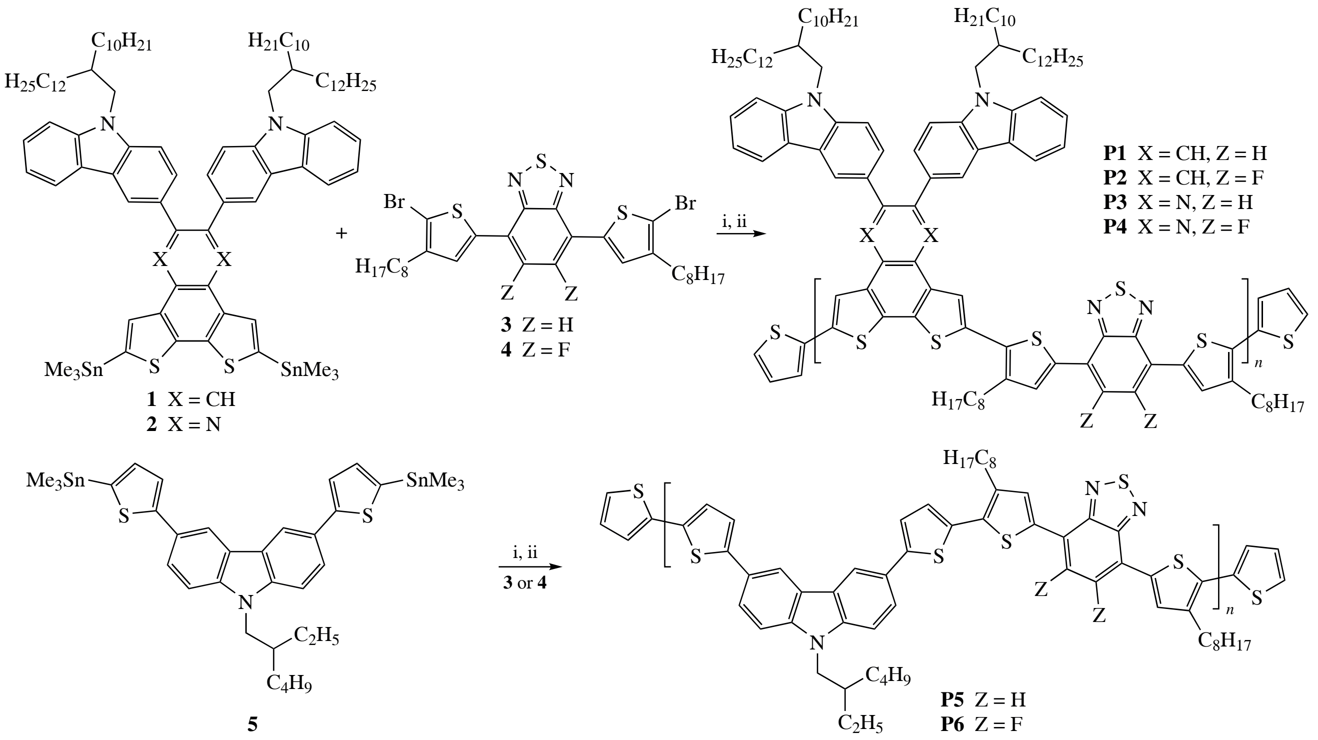

Scheme 1 *Reagents and conditions*: i, $Pd_2(dba)_3$, (*o*-$MeC_6H_4)_3P$, toluene, reflux, 5 h; ii, 2-(trimethylstannyl)thiophene, then 2-bromothiophene (excess).

a set of solvents: heptane, acetone, dichloromethane, chlorobenzene, and 1,2-dichlorobenzene when necessary. Usually, the target fraction was collected from the chlorobenzene or 1,2-dichlorobenzene extracted solutions. The relative molecular weight characteristics of the polymers **P1–P6** are listed in Table 1. Thermal properties of polymers **P1–P6** were studied using thermogravimetric analysis (TGA) and differential scanning calorimetry (DSC). As an example, Figure S1 (see Online Supplementary Materials) shows the thermal gravimetry plot for polymer **P1**, which demonstrates a single-stage thermal decomposition at a temperature of about 474 °C, accompanied by a loss of ~82% of its weight. No signals were recorded on the DSC curves for the obtained polymers, indicating their amorphous state. All the obtained polymers demonstrated high thermal stability. However, when comparing polymers containing fluorinated and non-fluorinated benzothidiazole fragments, it can be noticed that the decomposition temperature (T_d) corresponding to 5% weight loss is somewhat higher for fluorinated polymers (see Table 1).

The optical properties of the obtained polymers **P1–P6** were studied in solution and in thin films using optical UV-VIS spectroscopy (Figure S2). The UV-VIS spectra of the obtained polymers exhibit major absorption bands in the range from 550 to 616 nm, which is associated with intramolecular charge transfer between donor and acceptor fragments. For polymers **P2**, **P4**, **P5**, and **P6**, the absorption bands have 'shoulders', which is probably associated with the aggregation of macromolecules in the solvent at room temperature [see Figure S2(*a*)]. The absorption spectra of the polymer films, in general, match well the corresponding spectra in solution [see Figure S2(*b*)]. It should be noted that the absorption spectra of some polymers show a considerable broadening in solid state as compared with their spectra in solution, which indicates strong intermolecular electronic interactions in the films. The band gap values (E_g^{opt}) for polymers **P1–P6** were determined using the Tauc method[26] [see Figure S2(*c*)] and vary within the range of 1.70–1.79 eV. The lowest value of 1.70 eV was obtained for polymer **P1**. The photoluminescence band maxima for thin films of **P1–P6** appear at 1.61–1.65 eV [see Figure S2(*d*)], which is close to the band gap values of these materials extracted from the absorption spectra.

The highest occupied molecular orbital (HOMO) energies were estimated for the obtained polymers **P1–P6** from the cyclic voltammetry measurements (Figure S3) performed for thin films. A standard approach[27] was used to estimate the HOMO energy value from the onset of the oxidation wave using the following equation:

$$E_{HOMO} = -[E^{ox}_{onset}\ vs.\ (Fc^+/Fc) + 4.8]\ (eV).$$

The energies of the lowest unoccupied molecular orbital (LUMO) of the polymers were estimated as $E_{LUMO} = E_g^{opt} + E_{HOMO}$ (eV). The obtained data presented in

Table 1 Physicochemical properties of polymers **P1–P6**.

Polymer	M_w/kDa[a]	M_w/M_n[b]	T_d/°C[c]	λ^{sol}_{max} (λ^{film}_{max})/nm[d]	E_g^{opt}/eV[e]	PL_{max}/eV[f]	E^{ox}_{onset}/V[g]	HOMO (LUMO)/eV[h]
P1	39	2.24	392	594 (614)	1.73	1.61	0.48	–5.28 (–3.55)
P2	92	1.97	396	603 (602)	1.78	1.65	0.44	–5.24 (–3.46)
P3	75	2.31	394	575, 591, 616 (606)	1.76	1.62	0.64	–5.44 (–3.68)
P4	37	1.12	423	557 (588)	1.79	1.62	0.55	–5.35 (–3.56)
P5	9	2.09	401	548 (575)	1.85	1.63	0.33	–5.13 (–3.28)
P6	28	1.26	444	555 (560)	1.84	1.62	0.30	–5.10 (–3.26)

[a] Weight-average molecular weight. [b] Polydispersity index. [c] Temperature corresponding to the 5 mass% loss. [d] Absorption maxima of polymers in solution/thin film. [e] Optical energy bandgap was estimated by Tauc plots derived from thin films absorption spectra. [f] Photoluminescence spectra of polymers in thin films. [g] Onset of the oxidation wave, *vs*. Fc^+/Fc. [h] HOMO energy was estimated from CV measurements and LUMO energy was estimated as E_g^{opt} + HOMO.

Table 1 demonstrate that the lowest HOMO and LUMO energies of about –5.40 eV and about –3.60 eV, respectively, were obtained for the pair of polymers **P3** and **P4** containing a dithienoquinoxaline fragment. The highest HOMO and LUMO energies of *ca.* –5.10 and –3.30 eV, respectively, were obtained for the pair of polymers **P5** and **P6** incorporating the *N*-alkylcarbazole fragment integrated within the polymer backbone.

At the next stage, we have investigated the photostability of the synthesized polymers **P1**–**P6** and the reference polymers PCDTBT and **P7** (Figure 1) under exposure to the mercury lamp UV light with the incidence of *ca.* 30 mW cm^{-2}. We emphasize that the experiment has been performed inside a nitrogen-filled glove box with well-controlled anoxic conditions (levels of O_2 and H_2O below 0.1 ppm), so the aging dynamics of the polymer films represent their intrinsic photostability behavior. The detailed description of the used setup, spectrum of the light source, and the methodology of the experiment were described previously.[19–21] Briefly, the thin polymer films (initial absorbance below 0.5) undergo light-induced degradation mainly due to the intermolecular cross-linking *via* the [2+2] cycloaddition pathway. As a consequence, the size of their conjugated π-systems becomes continuously reduced, which results in the blue shift of the absorption band and overall decay in the film absorbance. This kind of behavior is illustrated for **P1** and the reference PCDTBT polymers in Figure 1(*a*). The light-induced cross-linking of polymer chains also generates defects, which facilitate non-radiative recombination of the photogenerated charge carriers (and also quenching of non-dissociated excitons). Therefore, the intensity of the photoluminescence (PL) of the polymer films also shows a rapid decay upon exposure of the materials to UV light [see Figure 1(*b*)].

The key parameter to analyze the aging behavior of polymer films is the evolution of the normalized film absorbance at the wavelengths corresponding to the band maxima for the pristine (non-aged) films as the function of the aging time. This approach allows one to visualize and compare the aging dynamics of all studied materials as shown in Figure 1(*c*). One could notice very fast photobleaching of the reference polymer **P7** [Figure 1(*d*)], so its normalized absorbance rapidly decays within the first 20–40 h of UV light exposure. It should be mentioned that **P7** has a structure very similar to that of the studied polymers, except for the presence of a highly popular benzodithiophene unit instead of the carbazole-loaded blocks in **P1**–**P6**. Another reference polymer, PCDTBT, is known as one of the most stable conjugated polymers ever designed.[28–30] Therefore, it is not surprising that it shows much slower aging dynamics in comparison with **P7**. Very similar aging behavior was demonstrated by our new polymers **P6**, **P2**, and **P5**, even though two last polymers were notably better than PCDTBT in terms of photostability. At the same time, polymers **P1**, **P3** and **P4** have shown much higher photostability than PCDTBT, which is reflected by the higher normalized absorbance of their films after 100 h of aging [see Figure 1(*c*)]. The highest photostability of **P1** is also reflected by the slower decay of its UV-VIS absorption and photoluminescence spectra, as clearly seen from Figure 1(*a*),(*b*).

To summarize, the previously performed studies for several groups of conjugated polymers[19–21] allowed us to identify some important relationships between the peculiarities of the material molecular structures and their photostability. Using these findings as a guideline, in this work we have rationally designed and synthesized a series of six conjugated polymers that demonstrated outstanding photostability. Five polymers outperformed PCTDBT, which has been an unbeatable polymer stability benchmark in the organic photovoltaics field for almost 20 years.[28–30] These new polymers may be considered as highly promising electron donor materials for a new generation of organic solar cells that are expected to deliver both high efficiency and long-term operational lifetimes. The designed polymers also have the big advantage of relatively simple molecular structures with a potential for scalable and low-cost synthesis, which is crucially important for the practical implementation of organic solar cells. In other contexts, the revealed excellent UV light hardness of the designed conjugated polymers makes them particularly promising for aerospace applications, *e.g.*, as components of solar cells for spacecraft, satellites, and other equipment for high-altitude missions where UV light and ionizing radiation severely affect the device operational lifetime.

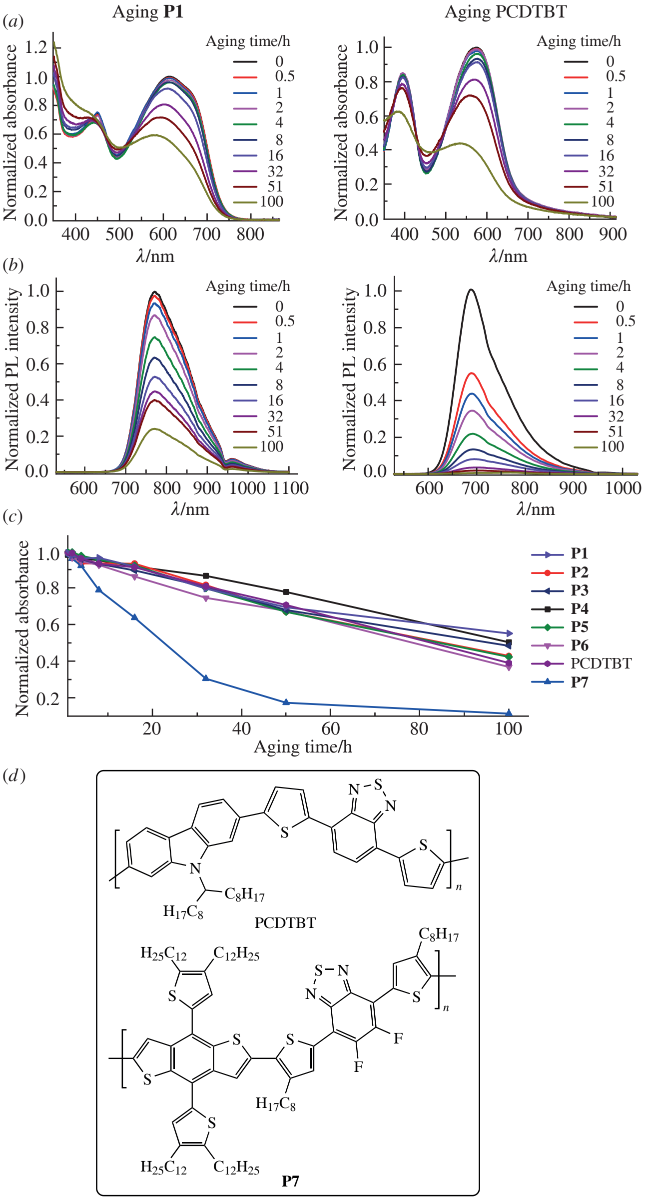

Figure 1 Evolution of the (*a*) absorption and (*b*) photoluminescence spectra of the polymers **P1** and PCDTBT upon exposure to hard UV light in an inert nitrogen atmosphere. (*c*) Dynamics of the normalized absorbance at the absorption band maximum of the polymer films depending on the aging time. (*d*) Molecular structures of the reference polymers **P7** and PCDTBT.

This work was supported by The Russian Science Foundation (grant no. 22-43-04427).

Online Supplementary Materials

Supplementary data associated with this article can be found in the online version at doi: 10.71267/mencom.7708.

References

1 L. Zhu, M. Zhang, G. Zhou, Z. Wang, W. Zhong, J. Zhuang, Z. Zhou, X. Gao, L. Kan, B. Hao, F. Han, R. Zeng, X. Xue, S. Xu, H. Jing, B. Xiao, H. Zhu, Y. Zhang and F. Liu, *Joule*, 2024, **8**, 3153; https://doi.org/10.1016/j.joule.2024.08.001.

2 L. Zhu, M. Zhang, Z. Zhou, W. Zhong, T. Hao, S. Xu, R. Zeng, J. Zhuang, X. Xue, H. Jing, Y. Zhang and F. Liu, *Nat. Rev. Electr. Eng.*, 2024, **1**, 581; https://doi.org/10.1038/s44287-024-00080-3.

3 J. Fu, Q. Yang, P. Huang, S. Chung, K. Cho, Z. Kan, H. Liu, X. Lu, Y. Lang, H. Lai, F. He, P. W. K. Fong, S. Lu, Y. Yang, Z. Xiao and G. Li, *Nat. Commun.*, 2024, **15**, 1830; https://doi.org/10.1038/s41467-024-46022-3.

4 P. Ding, D. Yang, S. Yang and Z. Ge, *Chem. Soc. Rev.*, 2024, **53**, 2350; https://doi.org/10.1039/D3CS00492A.

5 X. Lu, C. Xie, Y. Liu, H. Zheng, K. Feng, Z. Xiong, W. Wei and Y. Zhou, *Nat. Energy*, 2024, **9**, 793; https://doi.org/10.1038/s41560-024-01501-1.

6 J. Sun, D. Li, J. Zou, S. Zhu, C. Xu, Y. Zou, Z. Zhang and H. Lu, *npj Comput. Mater.*, 2024, **10**, 181; https://doi.org/10.1038/s41524-024-01367-7.

7 M. Li and F. He, *Next Energy*, 2024, **2**, 100085; https://doi.org/10.1016/j.nxener.2023.100085.

8 P. Jiang, Y. Liu, J. Song and Z. Bo, *Acc. Chem. Res.*, 2024, **57**, 3419; https://doi.org/10.1021/acs.accounts.4c00592.

9 N. Yang, Y. Cui, Y. Xiao, Z. Chen, T. Zhang, Y. Yu, J. Ren, W. Wang, L. Ma and J. Hou, *Angew. Chem., Int. Ed.*, 2024, **63**, e202403753; https://doi.org/10.1002/anie.202403753.

10 M. Manceau, E. Bundgaard, J. E. Carlé, O. Hagemann, M. Helgesen, R. Søndergaard, M. Jørgensen and F. C. Krebs, *J. Mater. Chem.*, 2011, **21**, 4132; https://doi.org/10.1039/C0JM03105D.

11 A. Rivaton, A. Tournebize, J. Gaume, P.-O. Bussière, J.-L. Gardette and S. Therias, *Polym. Int.*, 2014, **63**, 1335; https://doi.org/10.1002/pi.4656.

12 S. Prasad, Z. Genene, C. F. N. Marchiori, S. Singh, L. K. E. Ericsson, E. Wang, C. M. Araujo and E. Moons, *Mater. Adv.*, 2024, **5**, 7708; https://doi.org/10.1039/D4MA00447G.

13 Z.-X. Liu, Z.-P. Yu, Z. Shen, C. He, T.-K. Lau, Z. Chen, H. Zhu, X. Lu, Z. Xie, H. Chen and C.-Z. Li, *Nat. Commun.*, 2021, **12**, 3049; https://doi.org/10.1038/s41467-021-23389-1.

14 A. I. Shames, L. N. Inasaridze, A. V. Akkuratov, A. E. Goryachev, E. A. Katz and P. A. Troshin, *J. Mater. Chem. A*, 2016, **4**, 13166; https://doi.org/10.1039/C6TA04605C.

15 L. N. Inasaridze, A. I. Shames, I. V. Martynov, B. Li, A. V. Mumyatov, D. K. Susarova, E. A. Katz and P. A. Troshin, *J. Mater. Chem. A*, 2017, **5**, 8044; https://doi.org/10.1039/C7TA00175D.

16 P. A. Troshin, D. K. Susarova, Y. L. Moskvin, I. E. Kuznetsov, S. A. Ponomarenko, E. N. Myshkovskaya, K. A. Zakharcheva, A. A. Balakai, S. D. Babenko and V. F. Razumov, *Adv. Funct. Mater.*, 2010, **20**, 4351; https://doi.org/10.1002/adfm.201001308.

17 I. V. Martynov, A. V. Mumyatov, L. G. Gutsev, L. N. Inasaridze, A. V. Kulikov and P. A. Troshin, *Adv. Funct. Mater.*, 2023, **33**, 2301637; https://doi.org/10.1002/adfm.202301637.

18 O. R. Yamilova, I. V. Martynov, A. S. Brandvold, I. V. Klimovich, A. H. Balzer, A. V. Akkuratov, I. E. Kusnetsov, N. Stingelin and P. A. Troshin, *Adv. Energy Mater.*, 2020, **10**, 1903163; https://doi.org/10.1002/aenm.201903163.

19 P. M. Kuznetsov, E. A. Komissarova, S. A. Kuklin and P. A. Troshin, *Mendeleev Commun.*, 2024, **34**, 338; https://doi.org/10.1016/j.mencom.2024.04.009.

20 P. M. Kuznetsov, I. V. Martynov, I. S. Zhidkov, L. G. Gutsev, E. A. Komissarova, A. V. Maskaev, A. I. Kukharenko, F. A. Prudnov and P. A. Troshin, *J. Phys. Chem. B*, 2023, **127**, 6432; https://doi.org/10.1021/acs.jpcb.3c03242.

21 P. M. Kuznetsov, I. V. Martynov, I. S. Zhidkov, L. G. Gutsev, E. A. Khakina, E. N. Zakharchenko, N. A. Slesarenko, A. I. Kukharenko and P. A. Troshin, *J. Mater. Chem. A*, 2023, **11**, 9019; https://doi.org/10.1039/D2TA09402A.

22 J.-Q. Pan, J.-P. Yi, G. Xie, W.-Y. Lai and W. Huang, *J. Phys. Chem. C*, 2018, **122**, 21569; https://doi.org/10.1021/acs.jpcc.8b05273.

23 N. V. Kravets, L. V. Kulik, V. A. Zinovyev and M. N. Uvarov, *Chem. Phys. Lett.*, 2024, **857**, 141698; https://doi.org/10.1016/j.cplett.2024.141698.

24 M. L. Keshtov, S. A. Kuklin, D. Yu. Godovskii, I. O. Konstantinov, M. M. Krayushkin, A. S. Peregudov and A. R. Khokhlov, *Dokl. Chem.*, 2016, **467**, 94; https://doi.org/10.1134/S0012500816030022.

25 I. Osaka, M. Shimawaki, H. Mori, I. Doi, E. Miyazaki, T. Koganezawa and K. Takimiya, *J. Am. Chem. Soc.*, 2012, **134**, 3498; https://doi.org/10.1021/ja210687r.

26 P. R. Jubu, F. K. Yam, V. M. Igba and K. P. Beh, *J. Solid State Chem.*, 2020, **290**, 121576; https://doi.org/10.1016/j.jssc.2020.121576.

27 C. M. Cardona, W. Li, A. E. Kaifer, D. Stockdale and G. C. Bazan, *Adv. Mater.*, 2011, **23**, 2367; https://doi.org/10.1002/adma.201004554.

28 W. R. Mateker, I. T. Sachs-Quintana, G. F. Burkhard, R. Cheacharoen and M. D. McGehee, *Chem. Mater.*, 2015, **27**, 404; https://doi.org/10.1021/acs.chemmater.5b02341.

29 C. H. Peters, I. T. Sachs-Quintana, J. P. Kastrop, S. Beaupré, M. Leclerc and M. D. McGehee, *Adv. Energy Mater.*, 2011, **1**, 491; https://doi.org/10.1002/aenm.201100138.

30 S. Beaupré and M. Leclerc, *J. Mater. Chem. A*, 2013, **1**, 11097; https://doi.org/10.1039/C3TA12420G.

Received: 12th December 2024; Com. 24/7708